Detection of Invasive Pulmonary Aspergillosis in Mice Using Lung Perfusion Single-Photon Emission Computed Tomography with [^{99m}Tc]MAA

Masataka Yoshida[1,2], Masato Tashiro[2,3*], Kodai Nishi[4], Maki Mishima[2], Kei Kawano[2,3], Takahiro Takazono[1,2], Tomomi Saijo[1,3], Kazuko Yamamoto[1,3], Yoshifumi Imamura[1,5], Taiga Miyazaki[1,2], Takashi Kudo[4], Katsunori Yanagihara[6], Hiroshi Mukae[1,5], Koichi Izumikawa[2,3]

[1]Department of Respiratory Medicine, Nagasaki University Hospital, Nagasaki, Japan

[2]Department of Infectious Diseases, Nagasaki University Graduate School of Biomedical Sciences, Nagasaki, Japan

[3]Nagasaki University Infection Control and Education Center, Nagasaki University Hospital, Nagasaki, Japan

[4]Department of Radioisotope Medicine, Atomic Bomb Disease Institute, Nagasaki University, Nagasaki, Japan

[5]Department of Respiratory Medicine, Nagasaki University Graduate School of Biomedical Sciences, Nagasaki, Japan

[6]Department of Laboratory Medicine, Nagasaki University Hospital, Nagasaki, Japan

Corresponding author: Masato Tashiro, MD, PhD

Department of Infectious Diseases, Nagasaki University Graduate School of Biomedical Sciences, 1-7-1 Sakamoto, Nagasaki 852-8501, Japan

Tel: +81-95-819-7731

Fax: +81-95-849-7766

E-mail: mtashiro@nagasaki-u.ac.jp

Running title: Lung Perfusion SPECT for Aspergillosis

Keywords: diagnosis; invasive pulmonary aspergillosis; perfusion single-photon emission computed tomography

Financial support

This work was supported by the Japan Society for the Promotion of Science (JSPS) KAKENHI Grant Number JP15K21230 and by the Program of the Network-Type Joint Usage/Research Center for Radiation Disaster Medical Science of Hiroshima University, Nagasaki University, and Fukushima Medical University.

ABSTRACT

There is an urgent need for development of better diagnostic strategies to improve outcomes in patients with invasive pulmonary aspergillosis (IPA). We hypothesized that lung perfusion single-photon emission computed tomography (SPECT) may be more sensitive and specific than computed tomography (CT) of the chest for detection of IPA because it is an angioinvasive pulmonary infection with characteristics that are different from those of bacterial pneumonia. We used SPECT with injection of technetium-99m-labeled macroaggregated albumin ([^{99m}Tc]MAA) to measure pulmonary perfusion in non-infected mice, mice with IPA, and mice with bacterial pneumonia. Histopathologic analysis was performed to evaluate the correlation between the perfusion defect and mold invasion. We also attempted to quantitatively evaluate the SPECT images to identify differences in decreased perfusion levels in affected areas in the mouse lung. Histopathologic analysis in the IPA mouse model showed a clear match between areas with a perfusion defect and the presence of mold, indicating that the location of the perfusion defect on a SPECT image reflects angioinvasion of the mold in the lungs. Some of these perfusion defects could be seen before appearance of the infiltrate of CT images. Quantitative analysis confirmed that perfusion in the affected areas was significantly decreased in the IPA model but not in the bacterial pneumonia model ($P < 0.0001$). This imaging method may be preferable to the alternative methods presently used to identify the presence of mold in a patient's lungs.

Introduction

Invasive pulmonary aspergillosis (IPA) is an opportunistic fungal infection caused by *Aspergillus* species. It is particularly common in patients with hematologic diseases and is often life-threatening in an immunocompromised host [1]. Despite treatment with currently available antifungal agents, the mortality of invasive aspergillosis reportedly remains as high as 30%–100% [2]. Therefore, there is an urgent need for development of better diagnostic strategies to improve the outcomes of this disease.

Early and accurate diagnosis of IPA, which is critical for better outcomes, remains a challenge. The diagnosis currently relies on culture methods, histopathology, and detection of diagnostic biomarkers (e.g., galactomannan and (1-3)-β-d-glucan) in serum or bronchoalveolar lavage fluid [3]. However, these procedures lack both sensitivity and specificity and can delay diagnosis. Further, invasive procedures cannot be used in patients who are seriously ill [4].

IPA is an angioinvasive pulmonary infection with characteristics that are different from those of bacterial pneumonia in spite of a similar clinical presentation and the infiltrates seen on computed tomography (CT) images. The initial findings typically include nodules with surrounding ground-glass opacities (i.e., the halo sign), which means hemorrhage in the area surrounding the fungus caused by invasion of the vasculature by *Aspergillus* hyphae [5]. The presence of halo sign allow the preemptive identification of IPA cases even before performing serum galactomannan test [6]. However, the halo sign is not specific for IPA, so is not considered to be definitive evidence of the disease [7].

Recently, Stanzani et al. suggested a potential role for CT pulmonary angiography in distinguishing between angioinvasive mold infection and other causes of pulmonary infiltrates, given its ability to detect angioinvasion [8]. Further, they observed that vessel

occlusion detected by CT pulmonary angiography was more sensitive than appearance of the halo sign. Although the number of patients in their study was small and the risk of nephrotoxicity associated with use of an intravenous contrast agent has not been adequately evaluated, their findings suggested that detection of angioinvasion would be an ideal way of identifying a focus of IPA in a patient's lungs earlier than would be possible using other clinical indicators.

Imaging modalities other than CT pulmonary angiography, such as single-photon emission computed tomography (SPECT), positron emission tomography (PET), and magnetic resonance imaging (MRI), can also be used for quantitative imaging of regional pulmonary perfusion [9]. SPECT in particular has several significant advantages. The technique most widely used when measuring pulmonary perfusion by SPECT involves injection of technetium-99m-labeled macroaggregated albumin ([^{99m}Tc]MAA). These particles are 10–150 μm in size and become lodged in the pulmonary capillaries at a rate that is proportional to local blood flow. Identification of the number of pulmonary capillaries destroyed by microinvasion of *Aspergillus* hyphae is necessary to be able to detect IPA in its early stages. Lung perfusion SPECT may be better able to identify IPA in its early stages than other modalities.

Several studies have attempted to develop a method to identify the localization of *Aspergillus* in the body. Petrik et al. reported that administration of ^{68}Ga-labeled siderophores, which are ferric ion-specific chelators, showed high uptake, specifically by *A. fumigatus* in vitro and in vivo, and therefore, could be used for PET imaging [10]. Wang et al. used ^{99m}Tc-labeled 28S fungal rRNA-targeted morpholino oligomer probes for in vivo SPECT imaging [11]. Recently, Rolle et al. developed a probe, [^{64}Cu]DOTA-labeled *A. fumigatus*-specific monoclonal antibody, and conducted in vivo antibody-guided PET and MRI [12]. These methods can aid the

direct visualization of locations of molds in the lungs, and their characteristics are ideal for the detection of IPA lesion. However, the safety of these experimental probes in humans has not been confirmed, and moreover, it use in routine clinical settings may be extremely expensive. A well-balanced usefulness and ease of access is important to familiarize the general population to these diagnostic modalities. Compared to these methods, lung perfusion SPECT is already well-established in routine clinical practice, is widely available, and is relatively inexpensive [9].

We hypothesized that lung perfusion SPECT may be more sensitive and specific than chest CT in its ability to detect IPA. In this study, lung perfusion SPECT/CT images of IPA and bacterial pneumonia were investigated in a mouse model to confirm our hypothesis.

Methods

Animals

Female ICR mice aged 6–8 weeks were purchased from Japan SLC, Inc. (Shizuoka, Japan). The animals were kept under standardized and sterile environmental conditions (room temperature 24°C, relative humidity 50%) on a 12-h light-dark cycle and received food and water ad libitum. All the animal experiments were performed in accordance with the recommendations in the Fundamental Guidelines for Proper Conduct of Animal Experiment and Related Activities in Academic Research Institutions under the jurisdiction of the Ministry of Education, Culture, Sports, Science and Technology. All experimental procedures were approved by the Institutional Animal Care and Use Committee of Nagasaki University (approval number 1408191168).

Mouse Model of IPA

The clinical isolate used in this experiment was *Aspergillus fumigatus* MF367, which was

obtained from the Pneumology Department of Nagasaki University Hospital, Nagasaki, Japan [13]. The fungus was grown on potato dextrose agar at 35°C until good sporulation was obtained. Conidia were harvested by flushing with sterile saline and subsequent filtering through a cell strainer with a pore size of 40 μm.

An intraperitoneal injection of cyclophosphamide (Sigma-Aldrich, St Louis, MO, USA; 150 mg/kg) was administered on day -3 and day 0 to render the animals neutropenic by day 5. On day 0, the mice were anesthetized by an intraperitoneal injection of medetomidine (Kyoritsu Seiyaku Corporation, Tokyo, Japan; 0.3 mg/kg), midazolam (Sandoz, Holzkirchen, Germany; 4.0 mg/kg), and butorphanol (Meiji Seika Pharma Co. Ltd., Tokyo, Japan; 5.0 mg/kg). The animals were then inoculated with 5×10^6 conidia of *A. fumigatus* MF367 via intratracheal injection [14]. Fifteen mice were sacrificed on days 4, 8, and 15 (five mice per group) to confirm that infection was successful. The lungs of these mice were collected in tubes with 1 mL of sterile saline and homogenized. Next, 100 μL of the cell suspensions were plated in 10-fold dilution steps on potato dextrose agar. The number of colony-forming units (CFU) were counted after 24–48 h of incubation at 35°C.

Mouse Model of Bacterial Pneumonia

A mouse model of bacterial pneumonia caused by the *Klebsiella pneumoniae* KEN-11 strain was used because of its good repeatability [15]. To prepare the inocula, a single colony of KEN-11 was incubated in Luria-Bertani broth at 37°C for 24 h with shaking at 250 rpm. ICR mice were intratracheally infected with the bacterial suspension (1×10^4 CFU/mouse) under general anesthesia using the method described above for the IPA model. No immunosuppression was needed for this model.

Ex Vivo Study

On comparison of lung perfusion SPECT images with pathologic findings, we realized that it would be impossible to compare SPECT images of living mice with pathologic images directly because the lungs collapsed and changed in shape when they were removed from the body. Therefore, we performed an ex vivo study as described below.

Approximately 80 MBq of [^{99m}Tc]MAA were administered via the tail vein on day 4 to mice infected with IPA (n = 5) and on day 3 to mice infected with bacterial pneumonia (n = 5). Ten minutes following the injection, the mice were sacrificed and the heart and both lungs were collected. The heart was not separated from the lungs to avoid dislodging [^{99m}Tc]MAA from the pulmonary capillaries. The organs were laid flat between sponges in labeled cassettes. The cassettes were then imaged using a Triumph combined PET/SPECT/CT system (TriFoil Imaging, Chatsworth, CA, USA). After imaging, the cassettes were fixed for processing, embedding, and sectioning. Tissue slices were stained with hematoxylin-eosin and Grocott's methenamine silver using standard procedures.

Imaging

The infected mice were imaged using the Triumph combined PET/SPECT/CT system. The SPECT images were acquired using a four-head gamma camera equipped with single pin-hole collimators (diameter 1.0 mm, focal length 90 mm). The experimental mice were injected in vivo with approximately 50 MBq of [^{99m}Tc]MAA via the tail vein. Immediately post-injection, the mice were anesthetized with isoflurane 1.5%. Approximately 5 minutes later, SPECT data were acquired for 21 minutes using the following imaging parameters: 20 s/projection, 64 projections over 360° in 5.6° increments, and a 40-mm radius of rotation. The CT images (X-ray source 75 kVp, 230 μA, 128 projections over 360°) were acquired after the SPECT images, with each animal in exactly the same position. All imaging work

was completed in the Radioisotope Research Center at Nagasaki University.

Analysis of SPECT/CT Images

The SPECT data were reconstructed using a three-dimensional (3D) maximum likelihood expectation maximization algorithm (50 iterations). The acquired SPECT and CT data were processed using the medical imaging data examiner tool in the AMIDE software package and OsiriX MD (Pixmeo, Geneva, Switzerland).

The SPECT images were quantitatively evaluated for 3D total lung volume and for the two-dimensional (2D) target lung area. For 2D analysis, we used maximum counts in the target region of interest (ROI) because most regions in a lung field include normal defects in the small pulmonary arterioles and capillary beds (e.g., the hilum of the lung, bronchus, and large vessels). A background ROI was also drawn in reference tissue that was outside the lung and presumed to be normal. The target-to-background ratio (TBR) was then calculated. For each 2D area, three TBR values (a target area and slices immediately above and below) were calculated. The mean TBR was calculated for each area. We compared the TBR value for the 3D total lung volume and that of the 2D affected area, defined as an area with an infiltrate on the CT image, for sequential changes from day 1 to day 5.

Mice in the two groups were compared to detect differences in decreasing perfusion levels in an affected area between lung tissue with IPA and that with bacterial pneumonia. The mean decrease (and the standard deviation) was calculated from the differences in TBR between areas with and without infiltrates on CT images in the lungs of mice in the IPA group (n = 10) and those in the bacterial pneumonia group (n = 5).

Statistical Analysis

Statistical significance was determined using the paired *t*-test. All tests were two-tailed, and a

P-value < 0.05 was considered statistically significant. The statistical analysis was performed using GraphPad Prism version 6.0 (GraphPad Software Inc., San Diego, CA, USA).

Results

Perfusion Defects in SPECT Images Indicate Angioinvasion by A. fumigatus

In this IPA mouse model, neutropenia (< 500 cells/μl) persisted to around day 5 and recovered after day 7. Therefore mice recovered from IPA after day 7. Before analysis of the perfusion SPECT images for the IPA mouse model, we confirmed the presence of *Aspergillus* in the lungs of the mice used in the study. The mean fungal burden (CFU/lung) was $1.1 \times 10^3 \pm 1.1 \times 10^3$ (day 4), $1.6 \times 10^1 \pm 1.5 \times 10^1$ (day 7), and $6.0 \times 10^0 \pm 1.3 \times 10^1$ (day 14), respectively (five mice per group). The fungal burden was highest on day 4 and gradually decreased from day 7 to day 14. A few Aspergilli remained in the lungs on day 14.

Lung perfusion SPECT with [^{99m}Tc]MAA in the normal mice provided clear images of the functional capillary beds in the lungs. Normal defects were seen, such as those in the hilum of the lung, bronchus, and large vessels, none of which contain small pulmonary arterioles. In the IPA mouse model, we found local abnormal defects in the lungs. Histopathologic analysis revealed inflammation, microvascular hemorrhage, and pulmonary alveolar edema in affected lung areas in the IPA mouse model on day 4 after infection (Fig. 1A, 1D). No necrotic areas were found on day 4 in the lungs of the mice used in this model, which suggests that the SPECT images in the ex vivo study were able to show IPA at a very early stage. We also confirmed that absence of lung perfusion on day 4 was not attributable to a necrotic change in the lung tissue. Images stained with Grocott's methenamine silver showed the elongated hyphal structures of the mold in the affected area (Fig. 1B, 1E). The pathologic analysis revealed micro-angioinvasion by *A. fumigatus* in affected areas. Other possible causes of

impaired pulmonary blood flow, such as pulmonary artery occlusion by *A. fumigatus*, were not observed.

A 2D perfusion SPECT image was reconstructed using the same slice as that used for pathologic analysis (Fig. 1C). The outline of the lungs seen on the perfusion SPECT image clearly matched that of the lung specimen. The same normal perfusion defects seen in the large pulmonary vessels and bronchus were detected on the in vivo images. We confirmed a local lung perfusion defect in the IPA mouse model, which could not be considered a normal defect because it included an area outside of the large vessels and bronchus (Fig. 1A, 1C). Further, there was a clear match between the perfusion defect area and the presence of *A. fumigatus* (Fig. 1B, 1C). The same results were obtained for all mice in the IPA model. These findings suggest that the perfusion defects identified on a SPECT image represent angioinvasion *of A. fumigatus* in the lungs and that the exact location of *A. fumigatus* can be determined during the early phase of IPA.

Sequential Changes on CT and perfusion-SPECT Images in an IPA Mouse Model

Physicians usually rely on chest radiographs and CT images to identify the location of mold infection in patients with suspected IPA. The sequential changes seen in our IPA mouse model were confirmed on CT images (Fig. 2). Most of the mice in this model showed no infiltrates on day 1 despite the presence of mold in their lungs. The infiltrates appeared from around day 5 after infection and persisted to around day 8, albeit with a slight reduction in density. The infiltrates had almost disappeared by approximately day 15, despite a few Aspergilli remaining. The sequential changes on perfusion SPECT images were also confirmed on CT images taken at the same times with the same positioning (Fig. 2). The same lesions that showed infiltrates on CT images also showed perfusion defects on the SPECT images. These perfusion defects persisted at around day 14 despite disappearance of

the infiltrate, indicating the possibility of residual *Aspergillus*, which would be consistent with the culture results showing some remaining *Aspergillus* at this time. Quantitative evaluation of the SPECT images on days 1 and 5 for the same mouse shown in Fig. 2 revealed a significant decrease in the TBR in the affected area, but did not show a significant decrease in 3D total lung volume (Fig. 3).

In some mice, we found abnormal areas with perfusion defects but no infiltrates on the CT images. Some of these perfusion defects appeared on day 1 and infiltrates subsequently appeared on day 5 in the same area (Fig. 4). However, we could not directly confirm the presence of mold at sites of perfusion defects without infiltrates because the lungs collapsed and changed in shape when they were removed from the body. These findings indicate that sites of IPA infection may be detected earlier on SPECT images than on CT images.

Perfusion SPECT Could Distinguish IPA From Bacterial Pneumonia

The ability to discriminate IPA from other types of pneumonia that could show similar infiltrates on CT images is important for selection of appropriate treatment. Therefore, we also performed CT and perfusion SPECT examinations in a mouse model of bacterial pneumonia. The pulmonary infiltrates seen on CT images on day 4 after infection in the IPA mouse model were also seen in the mouse model of bacterial pneumonia (Fig. 5A). It was impossible to distinguish between bacterial pneumonia and IPA on the CT images because the characteristics of the infiltrates were too similar.

We also assessed the ability of SPECT perfusion images to distinguish between bacterial pneumonia and IPA. Unlike the mice with IPA, most of the mice with bacterial pneumonia showed only a minor decrease in perfusion on SPECT images (Fig. 5A). A perfusion defect was detected in one of the mice in the ex vivo bacterial pneumonia study; however, this mouse had developed extremely severe pneumonia, so the defect was attributed to necrotic

changes in the lung. Most mice showed only a very slight decrease in perfusion similar to that in the in vivo study.

We also attempted to distinguish between IPA and bacterial pneumonia using differences in the TBR between an affected area and a normal area. TBR values could decrease for several reasons, including a reduction in the amount of [^{99m}Tc]MAA injected, so we did not directly compare these values between the lesions and instead compared them between areas with and without infiltrates. The difference in TBR between affected areas and normal areas was statistically significant (32.4 ± 5.6 for IPA [n = 10] and 7.1 ± 6.3 for bacterial pneumonia [n = 5]; $P < 0.0001$; Fig. 5B), indicating that perfusion in an affected area was significantly lower than that in a normal area in mice with IPA but not in mice with bacterial pneumonia.

Discussion

Aspergillus spp. are the causative organisms for IPA, which is associated with high morbidity and mortality, especially in allogeneic hematopoietic stem cell transplant recipients and patients with hematologic malignancies. When the spores are inhaled by patients who are neutropenic, they germinate and the hyphae invade the tissues [16]. *Aspergillus* spp. also invade and occlude the blood vessels, causing thrombosis and tissue infarction. Development of a method that can evaluate the blood vessels in the lung could allow earlier diagnosis of angioinvasive pulmonary mold disease [17]. Micro-angioinvasion would occur before tissue infarction, so a method that can evaluate micro-pulmonary perfusion could detect IPA earlier than CT pulmonary angiography. In this study, we demonstrated that perfusion SPECT with [^{99m}Tc]MAA could detect micro-angioinvasion by mold, so this well-established method has potential for earlier diagnosis of IPA. Moreover, compared with CT pulmonary angiography, perfusion SPECT should also be better able to detect infarcted lung tissue in patients with IPA

because it is also an established method for diagnosis of pulmonary infarction [18]. Unfortunately, this could not be investigated in our IPA mouse model because the mice had already succumbed to IPA before infarction could develop. However, clear perfusion defects attributable to tissue necrosis were seen in the mouse model of bacterial pneumonia, which suggests that impaired pulmonary blood flow could be detected by this method.

In this study, we showed two potential benefits of perfusion SPECT with [^{99m}Tc]MAA for detection of IPA. First is the potential for perfusion SPECT to detect IPA earlier than CT imaging, which is important considering that the earliest findings in patients with IPA at present are abnormalities on CT imaging. Despite the resolution of the preclinical SPECT system used in this study is much lower than CT, perfusion SPECT could detect the IPA infection early phase, as described in results. This is the evidence that perfusion SPECT has a very high sensitivity to IPA infection. The earlier treatment is started in these patients, the better the prognosis, so earlier diagnosis of IPA using perfusion SPECT might improve the outcomes of treatment [19]. Clinical trials are now needed to confirm that perfusion SPECT can detect IPA earlier than CT. Perfusion SPECT is already widely used in routine clinical practice and can be put to further practical use if physicians can agree on when perfusion SPECT should be considered in patients with suspected IPA. Second, we found that if a perfusion defect was present, it persisted on the CT images in spite of improvement with regard to the infiltrate. The clinical significance of such persistent defects is still not clear. However, given that we were able to confirm persistence of a perfusion defect and mold in the lungs of mice with IPA at the same time, it is possible that perfusion SPECT could help to guide decisions with regard to cessation of antifungal treatment. Unfortunately, we were not able to analyze the relationship between lung infiltrates, perfusion defects, and presence of mold in the lungs directly by invasive methods such as pathologic or culture analysis. The main reasons for this were that non-invasive CT imaging was required in the same mice over

time in this sequential imaging experiment and that it was impossible to perform CT imaging of lungs that had collapsed and changed in shape after removal from the body.

A possible concern regarding perfusion SPECT is its specificity for diagnosis of IPA. There are many clinical causes of impaired pulmonary perfusion, including embolization, infarction, necrosis, destruction of capillaries, and hypoxic pulmonary vasoconstriction. Hypoxic pulmonary vasoconstriction can be caused by any type of pneumonia and also by atelectasis in affected areas [20]. Blood flow in affected areas may be decreased to varying degrees depending on the severity of pneumonia. Although IPA and bacterial pneumonia have a similar clinical presentation, bacteria do not directly destroy pulmonary capillaries, whereas mold is angioinvasive, and the difference in extent of the perfusion decrease in the affected area between IPA and bacterial pneumonia was confirmed in our study. This difference indicates that perfusion SPECT can distinguish IPA from bacterial pneumonia and atelectasis, which show a variety of infiltrates on CT images. In addition, we continue to analyze the ability of perfusion SPECT to distinguish mold infection other than aspergillosis such as mucormycosis from IPA.

We observed a clear perfusion defect for severe bacterial pneumonia with necrosis in this study. This finding indicates that septic emboli and lung abscess, which are respective manifestations of embolization and tissue necrosis, may show a perfusion defect resembling that found in IPA. However, these differential diagnoses can usually be distinguished by host factors and the results of other examinations.

Another significant aspect of this study was that pulmonary perfusion could be quantified by SPECT imaging. Perfusion SPECT has rarely been used to image the lungs of small animals, so a quantitative method for measuring lung perfusion is not established. Generally, average values are often used for data analysis. However, we calculated TBR using the maximum

uptake counts in the ROIs in the present study. There are two reasons why it was not reasonable to adopt the average uptake counts to calculate the TBR. First, the ROIs include areas with normal perfusion defects, so lung perfusion is easily underestimated. Second, the distribution of [^{99m}Tc]MAA is not uniform. In using the maximum uptake values, we referred to the idea of maximum of standardized uptake value (SUV_{max}) which widely used for clinical PET examination. TBR calculated from maximum uptake value is little affected by scatter noise, non-uniformity of ^{99m}Tc-MAA, and normal perfusion defects. Thus, TBR allowed successful quantification of lung perfusion without the effects of areas containing normal defects and non-uniform tracer distribution.

In conclusion, we have found that lung perfusion SPECT with [^{99m}Tc]MAA can detect micro-angioinvasion by *A. fumigatus* in an IPA mouse model, indicating that this imaging technique could be used to identify the presence of the mold in a patient's lungs. This method has several advantages in that it will allow earlier detection of mold invasion, the examination is non-invasive, inexpensive, and without adverse effects for patients, and it is already in routine clinical use. We proceed clinical confirmation of these results in the future.

Funding This work was supported by the Japan Society for the Promotion of Science (JSPS) KAKENHI Grant Number JP15K21230 and by the Program of the Network-Type Joint Usage/Research Center for Radiation Disaster Medical Science of Hiroshima University, Nagasaki University, and Fukushima Medical University.

Conflicts of interest

All authors declare no conflicts of interest in this work.

Acknowledgments

We are grateful to Yuichiro Nakano and Minori Kikuchi for their technical assistance with this research.

References

1. Patterson TF, Thompson GR, 3rd, Denning DW, *et al.* Practice Guidelines for the Diagnosis and Management of Aspergillosis: 2016 Update by the Infectious Diseases Society of America. *Clin Infect Dis.* 2016; 63: e1-e60.
2. Verweij PE, Chowdhary A, Melchers WJ, Meis JF. Azole Resistance in Aspergillus fumigatus: Can We Retain the Clinical Use of Mold-Active Antifungal Azoles? *Clin Infect Dis.* 2016; 62: 362-8.
3. De Pauw B, Walsh TJ, Donnelly JP, *et al.* Revised definitions of invasive fungal disease from the European Organization for Research and Treatment of Cancer/Invasive Fungal Infections Cooperative Group and the National Institute of Allergy and Infectious Diseases Mycoses Study Group (EORTC/MSG) Consensus Group. *Clin Infect Dis.* 2008; 46: 1813-21.
4. Ambasta A, Carson J, Church DL. The use of biomarkers and molecular methods for the earlier diagnosis of invasive aspergillosis in immunocompromised patients. *Med Mycol.* 2015; 53: 531-57.
5. Primack SL, Hartman TE, Lee KS, Muller NL. Pulmonary nodules and the CT halo sign. *Radiology.* 1994; 190: 513-5.

6. Weisser M, Rausch C, Droll A, *et al.* Galactomannan does not precede major signs on a pulmonary computerized tomographic scan suggestive of invasive aspergillosis in patients with hematological malignancies. *Clin Infect Dis.* 2005; 41: 1143-9.

7. Lee YR, Choi YW, Lee KJ, *et al.* CT halo sign: the spectrum of pulmonary diseases. *Br J Radiol.* 2005; 78: 862-5.

8. Stanzani M, Sassi C, Lewis RE, *et al.* High resolution computed tomography angiography improves the radiographic diagnosis of invasive mold disease in patients with hematological malignancies. *Clin Infect Dis.* 2015; 60: 1603-10.

9. Hopkins SR, Wielputz MO, Kauczor HU. Imaging lung perfusion. *J Appl Physiol (1985).* 2012; 113: 328-39.

10. Petrik M, Haas H, Dobrozemsky G, *et al.* 68Ga-siderophores for PET imaging of invasive pulmonary aspergillosis: proof of principle. *J Nucl Med.* 2010; 51: 639-45.

11. Wang Y, Chen L, Liu X, *et al.* Detection of Aspergillus fumigatus pulmonary fungal infections in mice with (99m)Tc-labeled MORF oligomers targeting ribosomal RNA. *Nucl Med Biol.* 2013; 40: 89-96.

12. Rolle AM, Hasenberg M, Thornton CR, *et al.* ImmunoPET/MR imaging allows specific detection of Aspergillus fumigatus lung infection in vivo. *Proc Natl Acad Sci U S A.* 2016; 113: E1026-33.

13. Tashiro M, Izumikawa K, Hirano K, *et al.* Correlation between triazole treatment

history and susceptibility in clinically isolated *Aspergillus fumigatus*. *Antimicrob Agents Chemother.* 2012; 56: 4870-5.

14. Kawai S, Takagi Y, Kaneko S, Kurosawa T. Effect of three types of mixed anesthetic agents alternate to ketamine in mice. *Exp Anim.* 2011; 60: 481-7.

15. Harada Y, Morinaga Y, Kaku N, *et al.* In vitro and in vivo activities of piperacillin-tazobactam and meropenem at different inoculum sizes of ESBL-producing Klebsiella pneumoniae. *Clin Microbiol Infect.* 2014; 20: O831-9.

16. Dagenais TR, Keller NP. Pathogenesis of Aspergillus fumigatus in Invasive Aspergillosis. *Clin Microbiol Rev.* 2009; 22: 447-65.

17. Herbrecht R, Roedlich MN. Earlier diagnosis of angioinvasive pulmonary mold disease: is computed tomography pulmonary angiography a new step? *Clin Infect Dis.* 2012; 54: 617-20.

18. Fazio F, Wollmer P. Clinical ventilation-perfusion scintigraphy. *Clin Physiol.* 1981; 1: 323-37.

19. Nucci M, Nouer SA, Cappone D, Anaissie E. Early diagnosis of invasive pulmonary aspergillosis in hematologic patients: an opportunity to improve the outcome. *Haematologica.* 2013; 98: 1657-60.

20. Dunham-Snary KJ, Wu D, Sykes EA, *et al.* Hypoxic Pulmonary Vasoconstriction: From Molecular Mechanisms to Medicine. *Chest.* 2017; 151: 181-192.

FIGURE LEGENDS

FIGURE 1. Histopathologic images and an ex vivo perfusion SPECT image for the same slice of lung in a mouse model of invasive pulmonary aspergillosis on day 4 after infection. (A) Hematoxylin-eosin staining. (B) Grocott's methenamine silver staining. (C) An ex vivo perfusion-SPECT image. (D) High-power field image indicated by a yellow arrow in Fig. 1A. Hematoxylin-eosin staining. (E) High-power field image indicated by a yellow arrow in Fig. 1B. Grocott's methenamine silver staining. †Heart. Black bar, 100 μm. SPECT, single-photon emission computed tomography

FIGURE 2. Sequential changes on CT images and perfusion single-photon emission computed tomographic images of the chest in a mouse with invasive pulmonary aspergillosis. The same lesion clearly appears as a perfusion defect with an infiltrate on the CT image; however, the perfusion defect persisted at around day 14 despite disappearance of the infiltrate (arrows). CT, computed tomography; Perf, perfusion

FIGURE 3. Quantitative evaluation of perfusion single-photon emission computed tomographic images on days 1 and 5 for the same mouse shown in Fig. 2. (A) TBR values for three-dimensional total lung. (B) TBR values for the two-dimensional affected area of the lung. *$P < 0.01$. TBR, target-to-background ratio

FIGURE 4. An example of a perfusion defect appearing earlier than the infiltrate in a mouse model of invasive pulmonary aspergillosis. The perfusion defect appeared on day 1 (white circle) and the infiltrate subsequently appeared in the same lesion on day 5 (yellow circle). CT, computed tomography; Perf, perfusion

FIGURE 5. Difference between invasive pulmonary aspergillosis and bacterial pneumonia on perfusion SPECT images. (A) The arrow shows an infiltrate on the chest CT image of a mouse with bacterial pneumonia on day 4 after infection, for which there is only a slight decrease in perfusion on the SPECT image. (B) Difference in maximum TBR between affected and non-affected areas in mouse models of invasive pulmonary aspergillosis and bacterial pneumonia. The difference in the TBR between an affected area and a normal area was 32.4 ± 5.6 for invasive pulmonary aspergillosis (n = 10) and 7.1 ± 6.3 for bacterial pneumonia (n = 5). *$P < 0.0001$. CT, computed tomography; SPECT, single-photon emission computed tomography; TBR, target-to-background ratio

Figure 1

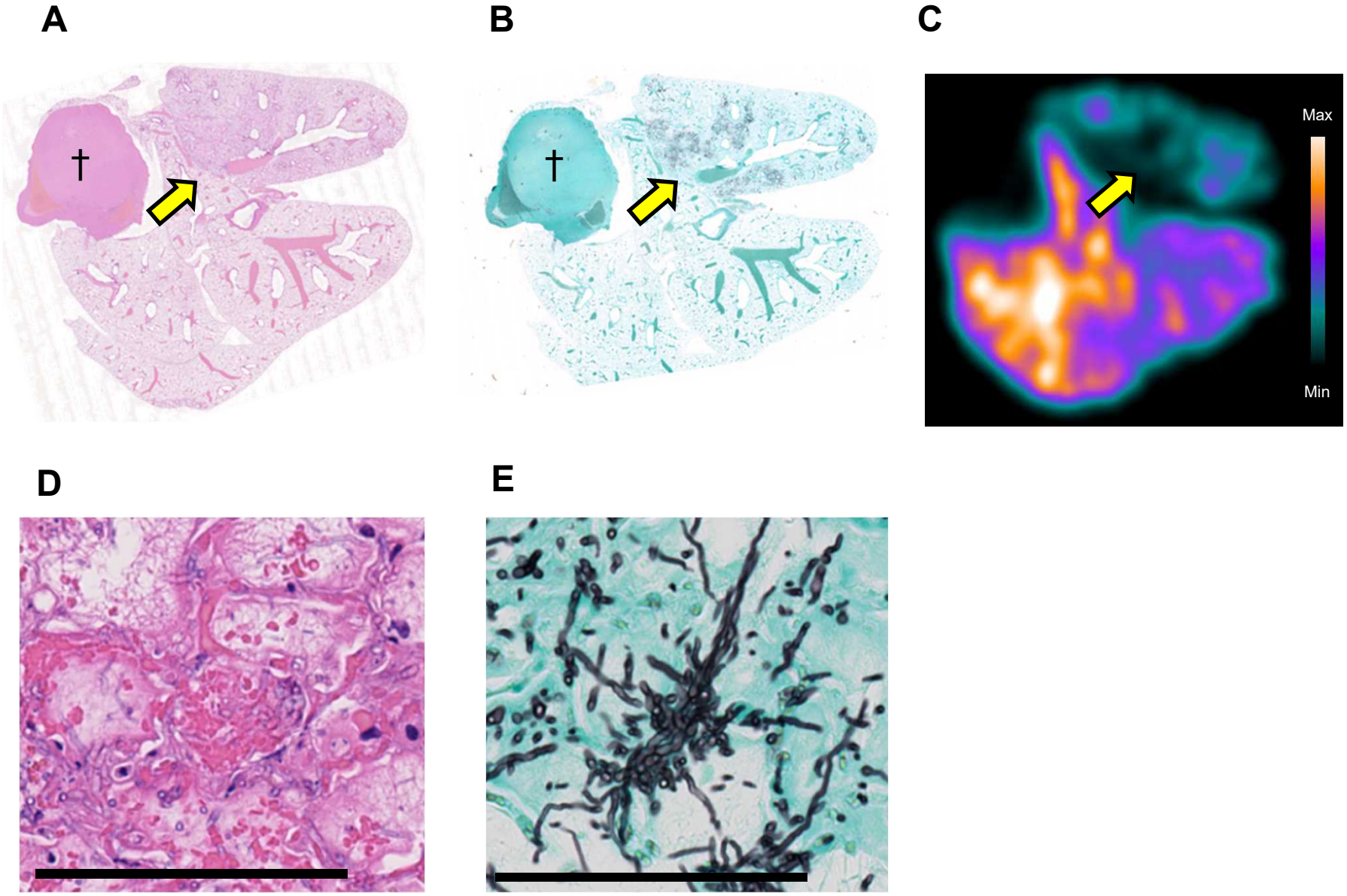

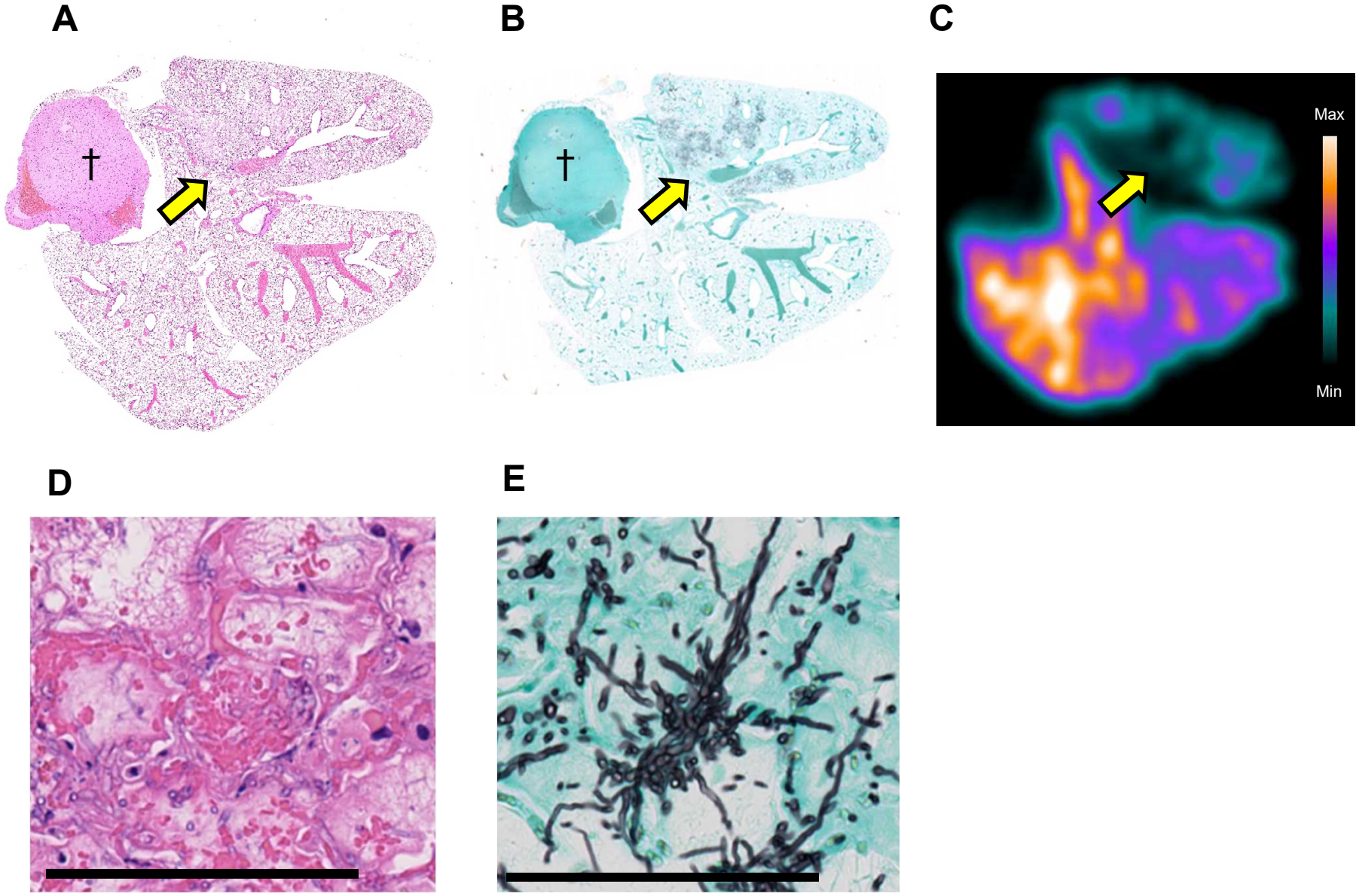
A
B
C
Max
Min
D
E

Figure 2

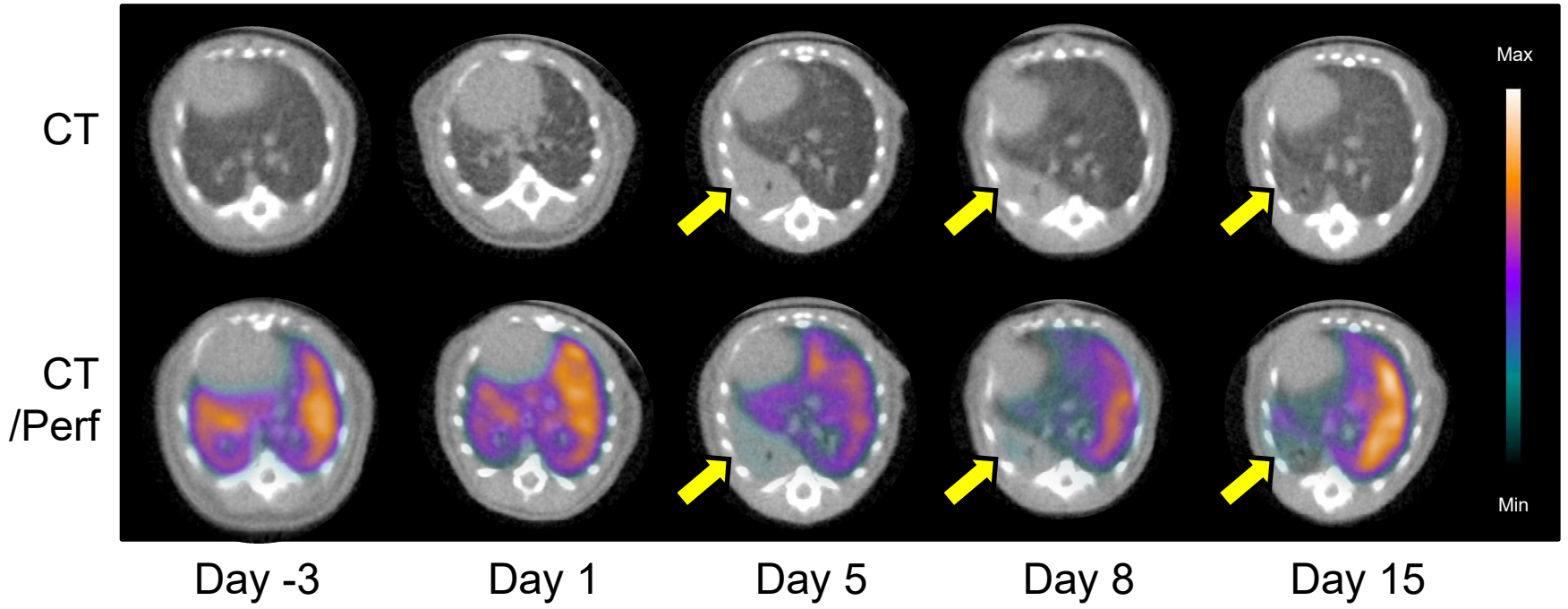

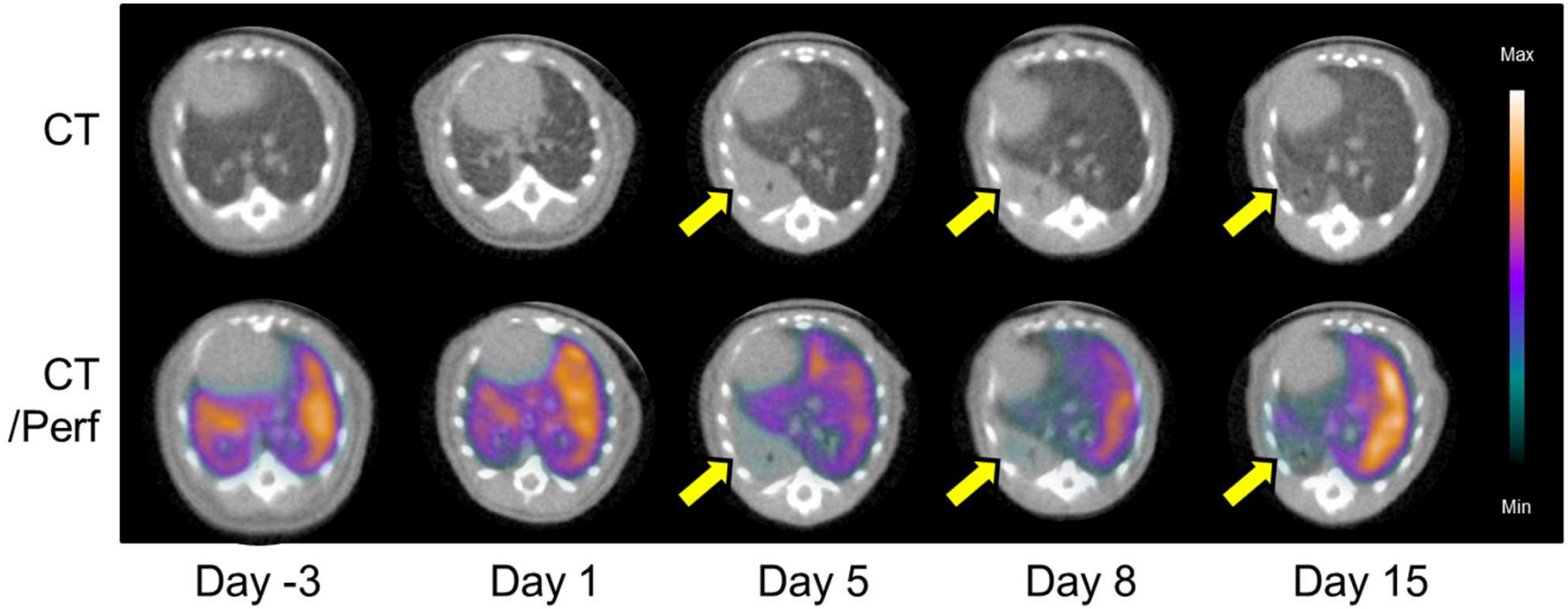
CT
CT
/Perf
Max
Min
Day -3
Day 1
Day 5
Day 8
Day 15

Figure 3

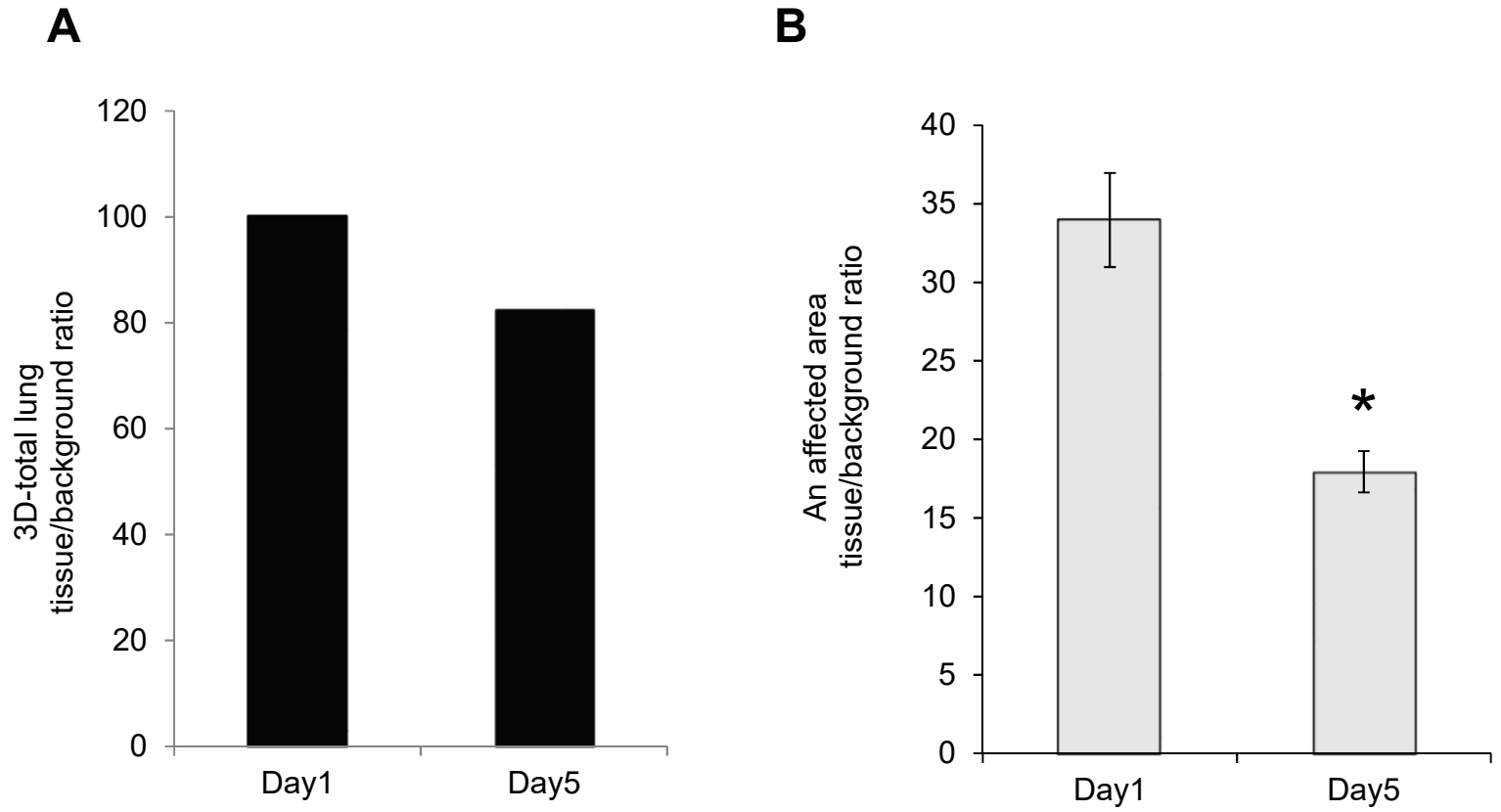
A
120
100
80
60
40
20
0
3D-total lung
tissue/background ratio
Day1
Day5
B
40
35
30
25
20
15
10
5
0
An affected area
tissue/background ratio
*
Day1
Day5

Figure 4

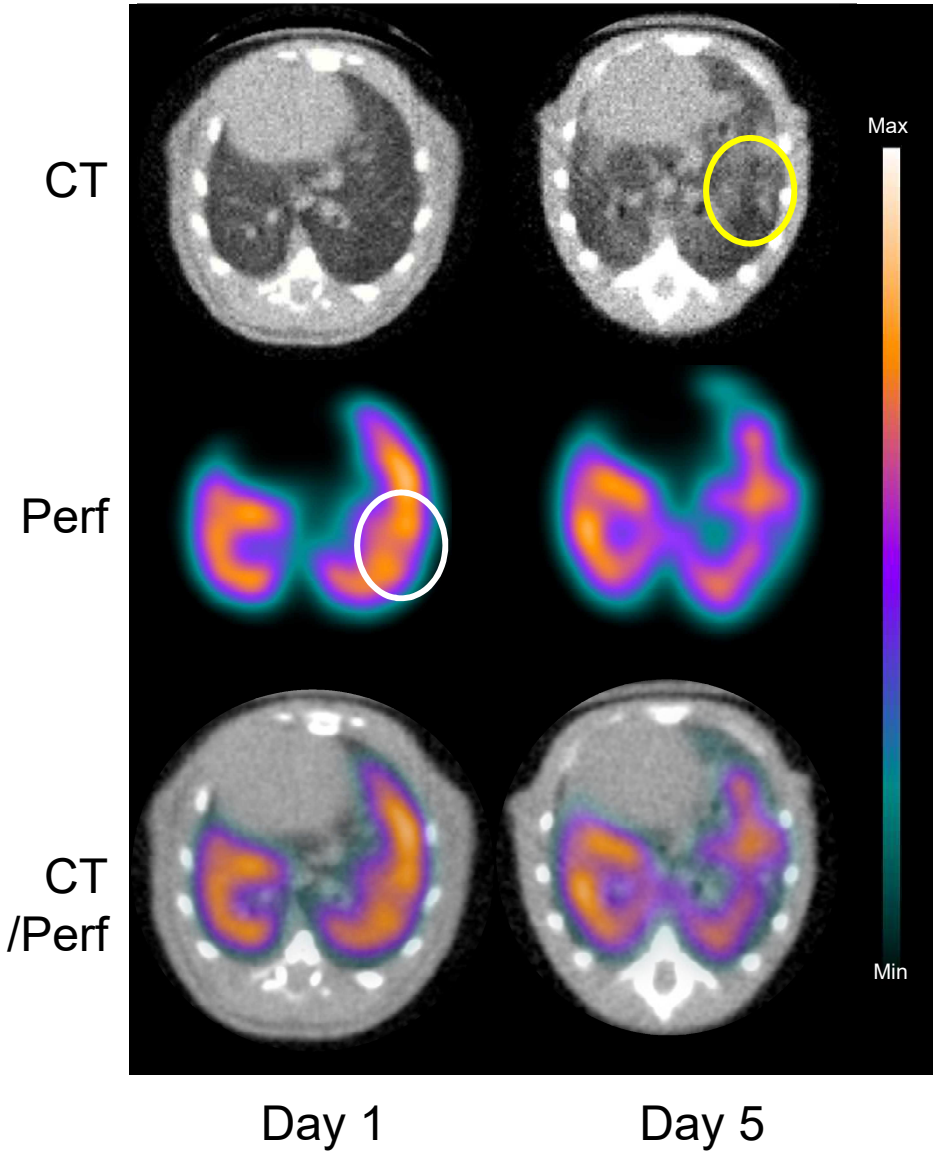

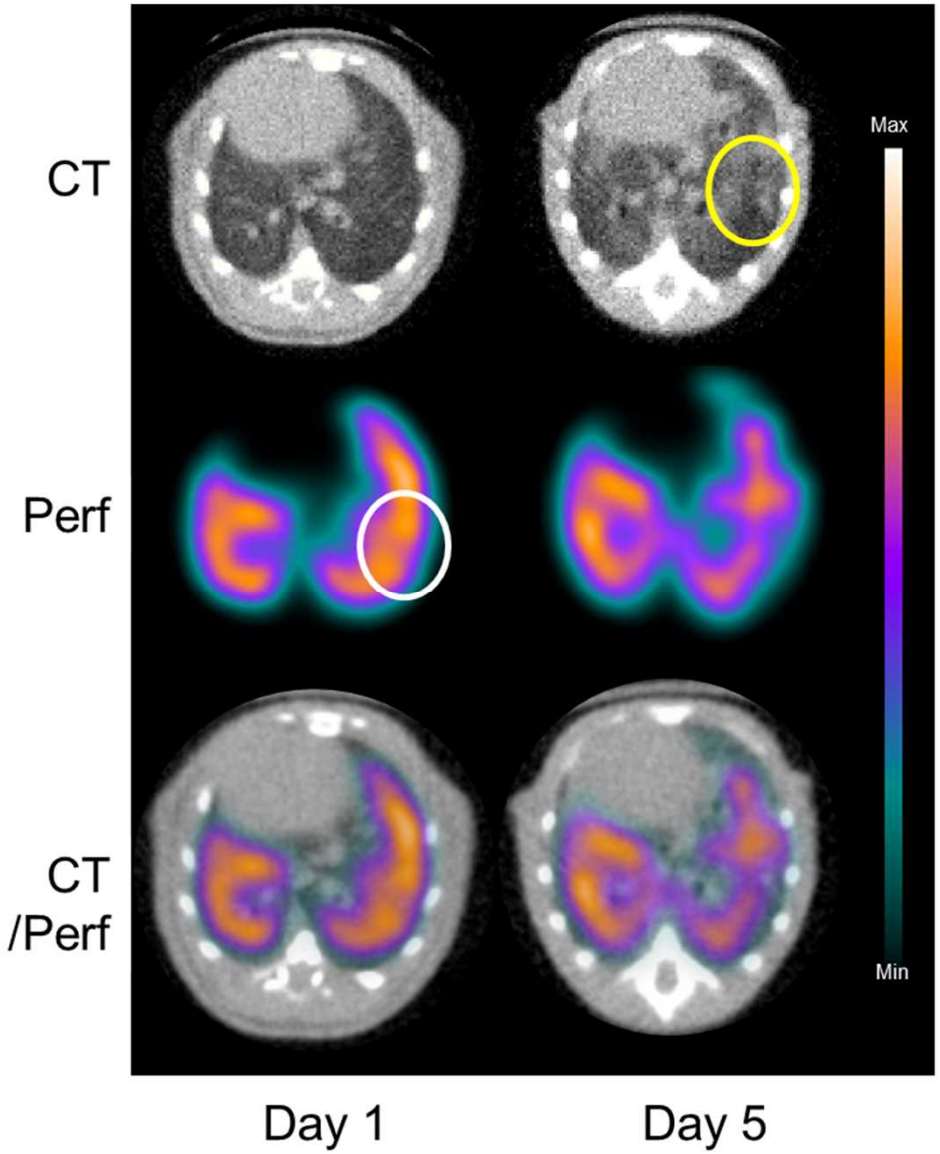
CT
Perf
CT
/Perf
Max
Min
Day 1
Day 5

Figure 5

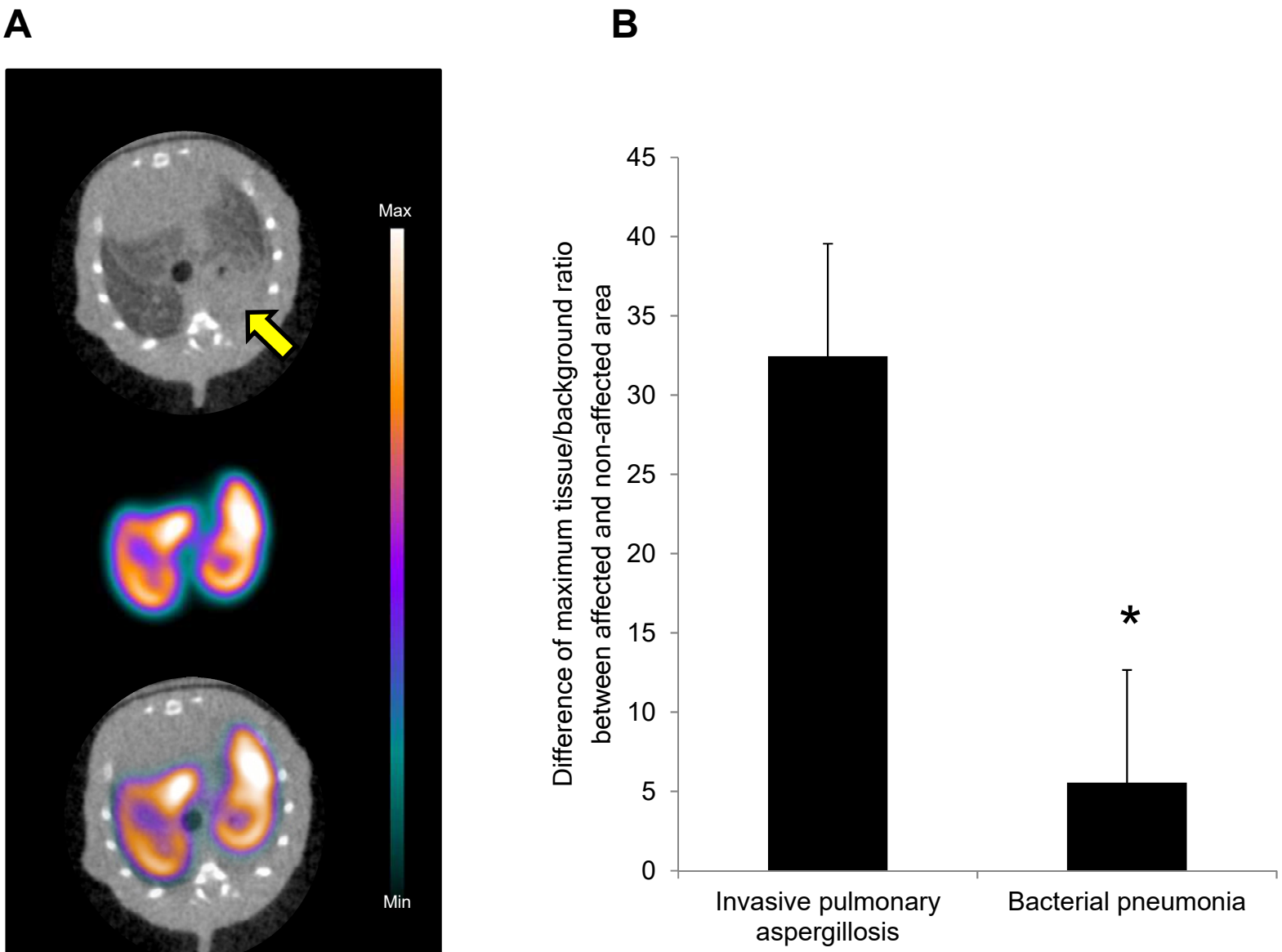
A
Max
Min
B
Difference of maximum tissue/background ratio between affected and non-affected area
45
40
35
30
25
20
15
10
5
0
*
Invasive pulmonary aspergillosis
Bacterial pneumonia

A

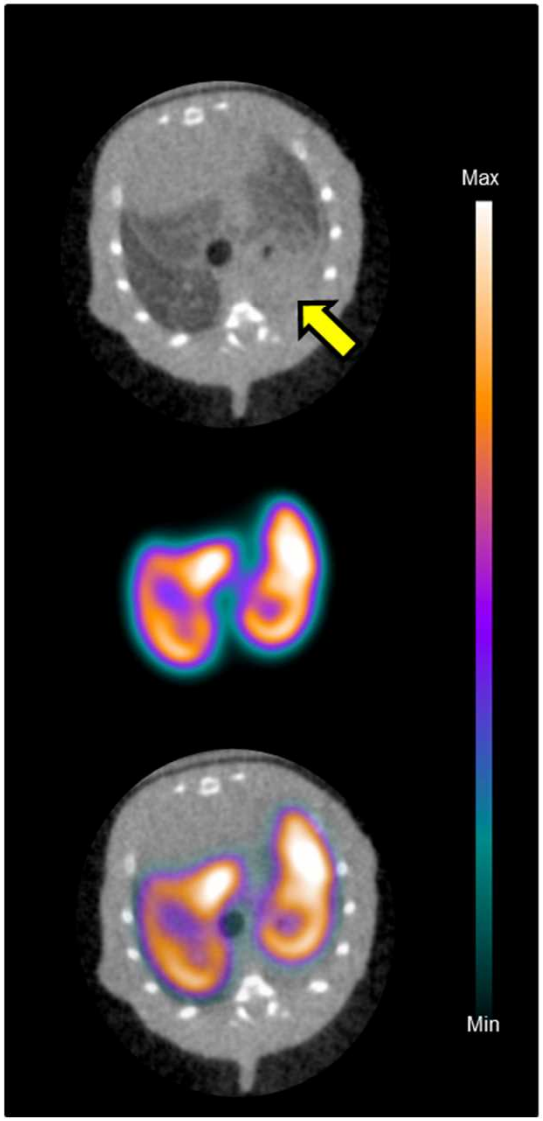
Max
Min

B

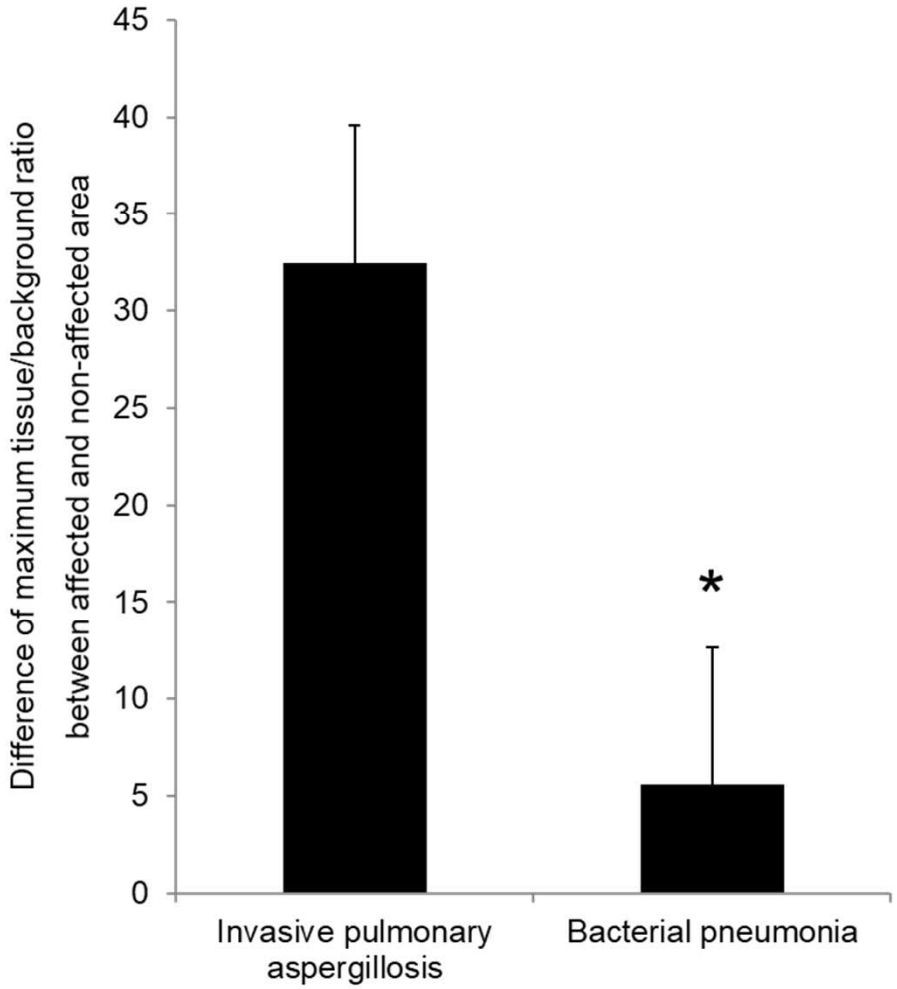
Difference of maximum tissue/background ratio between affected and non-affected area
45
40
35
30
25
20
15
10
5
0
*
Invasive pulmonary aspergillosis
Bacterial pneumonia